Clin Oral Invest (2012) 16:387–393
DOI 10.1007/s00784-011-0544-9

ORIGINAL ARTICLE

Assessment of variations of the mandibular canal through cone beam computed tomography

Christiano de Oliveira-Santos · Paulo Henrique Couto Souza · Soraya de Azambuja Berti-Couto · Lien Stinkens · Kristin Moyaert · Izabel Regina Fischer Rubira-Bullen · Reinhilde Jacobs

Received: 18 October 2010 / Accepted: 7 March 2011 / Published online: 30 March 2011
© Springer-Verlag 2011

Abstract The neurovascular bundle may be vulnerable during surgical procedures involving the mandible, especially when anatomical variations are present. Increased demand of implant surgeries, wider availability of three-dimensional exams, and lack of clear definitions in the literature indicate that features of anatomical variations should be revisited. The objective of the study was to evaluate features of anatomical variations related to mandibular canal (MC), such as bifid canals, anterior loop of mental nerve, and corticalization of MC. Additionally, bone trabeculation at the submandibular gland fossa region (SGF) was assessed and related to visibility of MC. Cone beam computed tomography exams from 100 patients (200 hemimandibles) were analyzed and the following parameters were registered: diameter and corticalization of MC; trabeculation in SGF region; presence of bifid MC, position of bifurcations, diameter, and direction of bifid canals; and measurement of anterior loops by two methods. Corticalization of the MC was observed in 59% of hemimandibles. In 23%, MC could be identified despite absence of corticalization. Diameter of MC was between 2.1 and 4 mm for nearly three quarters of the sample. In 80% of the sample trabeculation at the SGF was either decreased or not visible, and such cases showed correlation with absence of MC corticalization. Bifid MC affected 19% of the patients, mostly associated with additional mental foramina. Clinically significant anterior loop (>2 mm of anterior extension) was observed in 22–28%, depending on the method. Our findings, together with previously reported limitations of conventional exams, draw attention to the unpredictability related to anatomical variations in neurovascularization, showing the contribution of individual assessment through different views of three-dimensional imaging prior to surgical procedures in the mandible.

Keywords Cone beam computed tomography · Jaw bone neurovascularization · Mandibular canal · Bifid mandibular canal · Anterior loop of mental nerve · Anatomical variations

C. de Oliveira-Santos · P. H. C. Souza · S. de Azambuja Berti-Couto · L. Stinkens · K. Moyaert · R. Jacobs
Oral Imaging Center and Department of Periodontology, Katholieke Universiteit, Leuven, Belgium

C. de Oliveira-Santos · I. R. F. Rubira-Bullen
Bauru School of Dentistry, University of São Paulo, São Paulo, Brazil

P. H. C. Souza
School of Dentistry, Pontifical Catholic University of Paraná, Curitiba, Brazil

S. de Azambuja Berti-Couto
School of Dentistry, Pontifical Catholic University of Rio Grande do Sul, Porto Alegre, Brazil

C. de Oliveira-Santos (✉)
Rua Rodrigo Argolo, 57/403, 41940-220 Salvador, BA, Brazil
e-mail: oliveirachristiano@hotmail.com

Introduction

Mandibular canals (MC) are anatomical structures that extend bilaterally from the mandibular foramen to the mental foramen (MF) carrying the inferior alveolar nerves, arteries, and veins. Anatomical variations in the path of the MC, such as bifid MC and anterior loops of the mental nerve, among others, are not rare [1, 2]. The neurovascular bundle may be vulnerable during surgical procedures involving the mandible [3].

Prevalence of anterior loop is quite variable in the literature, occurring in between 28% and 71% of the samples studied [3–10], and their anterior extensions range from 0 to 9 mm [4–7, 10]. Lack of explicit definitions and standardized methods to assess their extension justifies revisiting the features of anterior loops, as well as other anatomical variations in the mandible.

Image quality of cone beam computed tomography (CBCT) systems and their relatively lower dose and cost when compared to conventional computed tomography have allowed more accessible three-dimensional assessment of craniofacial structures in dental practice [11]. CBCT has been shown superior to panoramic radiographs in displaying the MC and their variations. Further understanding of such anatomical variations is essential to the performance of more predictable surgical procedures, avoiding potential sensory disturbances, hemorrhagic complications, and even failures in anesthetic techniques [12].

The purpose of the present study is to assess the MC and its variations through CBCT images. Features of bifid MC and anterior loop of the mental nerve are reported. Additionally, corticalization of the MC and bone trabeculation in the submandibular gland fossa (SGF) region are assessed.

Methods

The sample consisted of 100 randomly selected CBCT exams, displaying the entire mandibular bone, scanned with Scanora 3D® (Soredex, Tuusula, Finland, high-resolution program, voxel size 0.2 mm), from patients (41 males, 59 females; 98 Caucasians, two non-Caucasians; 17 aged ≤20 years old, 27 between 21 and 40 years old, 34 between 41 and 60 years old, and 22 above 60 years old) referred for several clinical reasons. All images were visualized with the Ondemand 3D™ software (Version 1.0, CyberMed Inc, Seoul, Korea) by three trained and calibrated observers (one oral and maxillofacial radiologist and two dental graduates, all with 1–2 years of clinical experience with CBCT diagnosis). Eventual disagreements were discussed and consensus was reached.

Hence, 200 hemimandibles were evaluated and the following parameters were registered: diameter of MC in the first molar region (scores, not visible, 0–2, 2.1–4, and 4.1–6, >6 mm); corticalization of the MC in the first molar region (present or absent); trabeculation in the SGF region (normal, decreased—i.e., significant decrease in trabeculation as visually compared to adjacent regions, not visible, increased—e.g., osteosclerosis caused by chronic trauma/inflammation history); presence of bifid MC, position of bifurcations, diameter, and direction of bifid canals; and measurement of anterior loops. Descriptive statistical analysis was carried out. Chi-square test was applied to assess association between corticalization of the MC and trabeculation in the SGF region.

Axial, coronal, sagittal, panoramic reconstructions, cross-sections, and volume rendering were viewed to assess bifid MC. Diameter and corticalization of MC, as well as trabeculation in the SGF region, were assessed on cross-sections. Two different views were used for assessing anterior loops: panoramic reconstructions and cross-sections. For the panoramic reconstructions (Fig. 1), line a was drawn following the inferior margin of the mandible. Lines b and c were drawn perpendicular to a, passing through the anterior border of the mental foramen and anterior border of the anterior loop (corresponding to the starting point of the incisive canal), respectively [7, 10]. Anterior loop (d) corresponded to the shortest straight-line distance between b and c. Slice thickness of panoramic reconstructions varied in each hemimandibles, ranging from 5 to 20 mm, so that the entire course of the canal could be visualized, including the mental foramen, without impairing image superimposition. For the cross-sections, the anterior loop was determined by counting the number of sequential 1 mm slices displaying two round hypodense images (corresponding to the upper and lower segments of the MC, typically ending in an “8-like” shape anteriorly), from the anterior-most image of the mental foramen and start point of the incisive canal. Hence, measurements on panoramic reconstructions presented inferior mandibular border as a reference, while occlusal plane served as

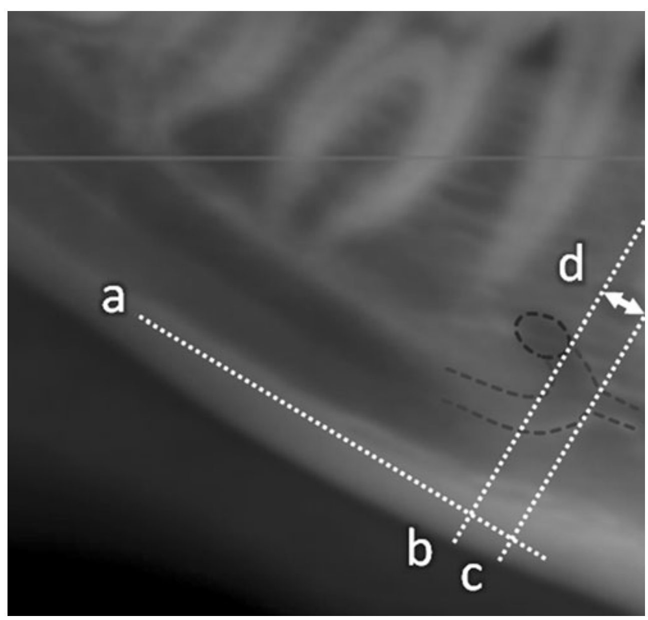

Fig. 1 Schematic representation of measurement of anterior extension of mental nerve anterior loop on reconstructed panoramic image. *a* Line tangenting inferior border of mandible, *b* line perpendicular to *a* tangenting anterior border of mental foramen, *c* line perpendicular to *a* tangenting the anterior-most part of mandibular canal, *d* anterior extension of anterior loop=shortest distance between *b* and *c*

reference on cross-sections (since those slices were reconstructed following the occlusal plane). Weighted Kappa index was calculated to assess agreement between observations on different views. For all the observations, Fisher and Chi-square tests were applied to compare right and left sides.

Results

No significant differences between genders, age groups, or left and right sides were observed for all parameters assessed.

On cross-sectional images of the first molar region, the corticalization of the MC was observed in the majority of hemimandibles (59%). In 23% of the cases the canal was not corticalized but could be visualized. The remainder (18%) could not be detected. The distribution of scores for width of the MC in the first molar region is presented in Table 1.

SGF regions showed either decreased trabeculation or not visible trabeculation in most hemimandibles (53% and 27%, respectively). Normal trabeculation was found in 15% and increased bone density was observed in 5% (Table 2). No correlation was found between trabeculation in the submandibular gland area and age or gender ($p=0.91$ and 0.51, respectively). Absence of MC corticalization was significantly correlated with decrease in trabeculation pattern in SGF region ($p<0.001$).

Bifid MC were observed in 19 patients (19%). Most of the bifurcations ($n=14$) were associated with additional mental foramina (AMF), with six cases of double mental foramina (i.e., diameter of AMF at least 50% of the corresponding mental foramen) and eight cases of accessory mental foramina (i.e., diameter of AMF less than 50% of the corresponding mental foramen). All bifurcations associated with AMF occurred in the body of the mandible, with six of these occurring in close proximity with the mental foramen (Fig. 2).

For the remaining bifid MC cases, not associated with AMF, the bifurcation was observed in the posterior region of the mandible, near the mandibular angle. In two cases the bifid canal rejoined the MC anteriorly to the bifurcation (Fig. 2). Three cases were observed with a bifid MC towards a retromolar foramen (Fig. 3). In two cases the bifid canal showed an upward curved direction, towards third molar region. The width of bifid MC (as measured at their widest portion) ranged between 1.03 and 3.3 mm (mean (SD)=1.5 (0.2) mm).

Presence and anterior extension of anterior loop of the mental nerve, as observed on panoramic reconstructions and cross-sections, are shown in Table 3. Agreement between observations on both views regarding presence/length of anterior loop was substantial (weighted Kappa index=0.71).

Table 1 Distribution of diameter scores for the mandibular canal in the first molar region

Diameter of MC	No.	Percent
0–2 mm	16	8
2.1–4 mm	148	74
4.1–6 mm	0	0
>6 mm	0	0
Not visible	36	18
Total	200	100

Discussion

Bifid mandibular canals

Bifid MC were observed in 19% of the patients in our sample. Previous studies with panoramic radiographs have reported incidences of less than 1% [13–15]. However, studies with CBCT images show much higher incidence, with reports from 15.6% to 65% [16, 17]. It has become clear that conventional radiographs are not reliable in detecting such anatomical variations.

Even among studies with 3D imaging, differences in incidence may be related to geographic/ethnical differences, as well as methodological discrepancies. In the present study, only bifid MC with diameter bigger than 1 mm were included, aiming clear clinical relevance of the results. Additionally, registration of “false mandibular canals” was carefully avoided. An image resembling a bifid MC may be produced by the imprint of the mylohyoid nerve on the internal mandibular surface [15]. Such images may mislead diagnosis, especially on panoramic reconstructions, which also highlights the importance of combining the different available reconstructions when assessing the mandibular anatomy.

Chavez-Lomeli et al. [18] described that the MC derives from three individual nerve branches from different origins at different stages of development. Further fusion of branches occurs, and bony canals develop around such nerve paths. During rapid prenatal growth and bone remodeling, there is a spread of intramembranous ossification that eventually forms the MC. This theory would explain the occurrence of bifid MC in some patients, secondary to incomplete fusion of these three nerves [15].

Diameter of bifid MC ranged between 1 and 3.3 mm (average 1.5 mm), and most main MC had between 2 and 4 mm of diameter. Previous studies [17] have found similar diameters for bifid MC (average 1.68 mm, range 0.9–3.4 mm) and main MC (average 3.3 mm, range 2.0–4.6 mm).

Several studies have proposed classifications to bifid MC. Nortjé et al. [12] and Langlais et al. [14], in retrospective studies with a large sample of panoramic

Table 2 Association between corticalization of mandibular canal and trabeculation pattern of the SGF region

Trabeculation n (% from total hemimandibles)	**Normal** 29 (15%)		**Decreased** 107 (53%)		**Not visible** 54 (27%)		**Increased density** 10 (5%)
Corticalization of Mandibular Canal	**Present**	**Not visible**	**Present**	**Not visible**	**Present**	**Not visible**	**Present**
Schematic representation	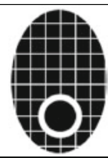	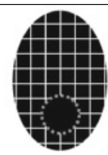		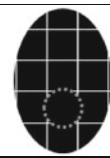	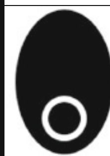	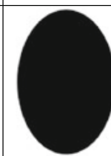	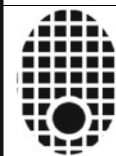
n (% by trabeculation)	23 (79%)	6 (21%)	67 (63%)	40 (37%)	18 (33%)	36 (67%)	10 (100%)

radiographs, proposed different classifications taking into consideration characteristics of the bifid canal such as association with additional mandibular foramen, relative width, and extension. In our study, as in previous studies with CBCT [17], no canals arising from separate mandibular foramina were found. Naitoh et al. [16] suggested the classification of bifid MC into four types, including buccolingual, forward, dental, and retromolar.

Three cases in our study presented retromolar canals associated with retromolar foramina. Sawyer and Kiely [19] observed retromolar foramina in 7.7% of adult mandibles and found a significant positive correlation with same-side occurrence of accessory mandibular foramen. In our study, however, none of the cases was associated with additional mandibular foramina. Bilecenoglu and Tuncer [20] found a prevalence of 25% for retromolar foramen and demonstrated histologically that those canals presented myelinated nerve fiber, artery, and numerous venules, and innervated part of third molar as well as mucosa in the retromolar area.

Bone trabeculation at submandibular gland fossa region

The SGF region encloses a depression in the lingual surface of the mandible which accommodates the submandibular gland and is usually seen on conventional radiographs as a diffuse radiolucent area in the posterior region of the mandible, inferior to the mylohyoid line [21]. In addition to the depth of the SGF, our results substantiate that in most cases bone trabeculation in that region may be significantly reduced when visually compared to other areas, or even not visible with 0.2 mm voxel size.

Visibility of the MC may vary between patients and even between different areas of the mandible. The canal is usually more readily identified in posterior areas and the visibility tends to decrease gradually towards the mental foramen [22]. Near the mental foramen, the MC has been shown to be "clearly visible" on CBCT cross-sections in around 53% to 65% of the cases [22, 23]. Similarly, a clear visibility of the MC in the first molar region may be found in 66% of the cases [22]. In the present study, the diameter of MC was measured

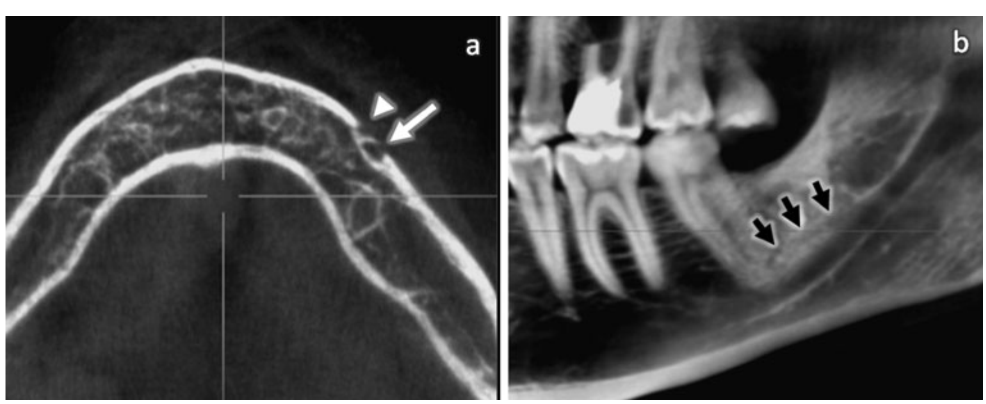

Fig. 2 **a** Bifurcation of mandibular canal associated with double mental foramen (*arrow head*), occurring near the mental foramen (*arrow*). **b** Bifid mandibular canal (*black arrows*) on the left mandibular body (cropped CBCT panoramic reconstruction, slice thickness 5 mm). The bifid canal rejoins the mandibular canal anteriorly to the bifurcation

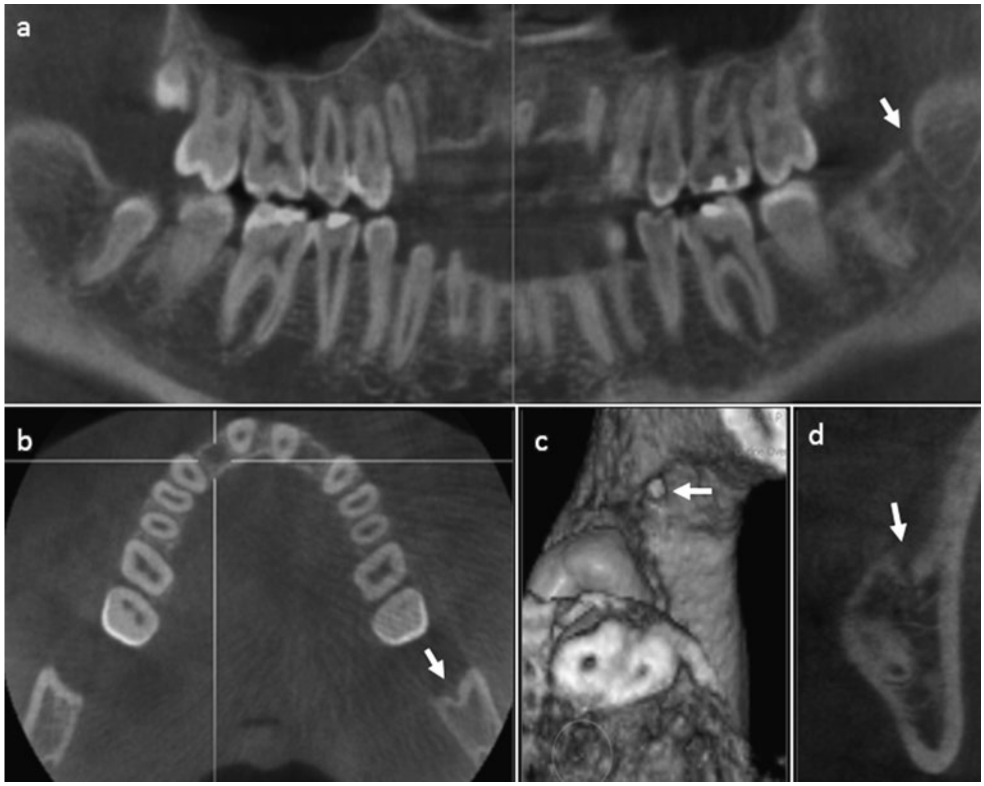

Fig. 3 Bifid mandibular canal towards retromolar foramen (*arrows*). **a** Panoramic reconstruction, **b** axial slice, **c** volume rendering (endoscopic function) showing retromolar region with foramen posterior to the third molar, and **d** cross-sectional image

on cross-sections in the first molar region, where in 18% of the cases the canal could not be visualized. This finding must be interpreted carefully, because only cross-sections were analyzed, and in one specific region. Combination with other views could have helped detect the MC. This demonstrates the importance of analyzing the different available views when assessing mandibular anatomy.

Additionally, bone trabeculation in SGF region, as observed in the present study, seems to influence the corticalization of MC. Visibility of the MC in the SGF region may be further affected by the absence of corticalization of the MC, which correlated with decreased bone trabeculation.

Anterior loop of the mental nerve

If proper preoperative evaluation is not carried out, patients with significant anterior extensions of mental nerve (anterior loop) are more likely to suffer from sensory disturbance or hemorrhagic complications when endosseous implants are installed in the most distal area of the interforaminal regions [7]. Depending on the method of measurement, between 22% and 28% of the hemimandibles presented significant anterior extension (2.1 mm or more). In 4–8% the anterior extension was larger than 4.1 mm.

Table 3 Distribution of scores for anterior loop of the mental nerve, as observed on panoramic CBCT reconstructions and cross-sections

Anterior loop	Panoramic *n* (%)	Cross-sections *n* (%)
Absent/up to 2 mm	135 (67)	136 (68)
Between 2.1 and 4 mm	39 (20)	33 (17)
Between 4.1 and 6 mm	14 (7)	7 (4)
Bigger than 6 mm	2 (1)	1 (<1)
Not clear/not visible	10 (5)	23 (11)
Total	200 (100)	200 (100)

Prevalence of anterior loop varies considerably in the literature. Anatomical studies with cadavers have reported prevalence ranging from 28% to 62.7% [3–7]. On panoramic radiographs, Ngeouw et al. [9] observed anterior loops in 40.2% of the mandibles. Kaya et al. [8] found 34% using spiral CT. A CBCT study reported 71% prevalence of anterior loop [10]. Anterior extensions ranging from 0 to 9.0 mm have been reported [3–7, 10]. Women [7, 10], older patients [7, 9], and shorter patients [9] may present smaller anterior extensions.

Despite some potential role of geographic variability in producing such discrepancies [2, 24], different methods for measurements and lack of a definitive definition of "anterior loop" seems to be recurrent in the literature. The anterior segment of the mental nerve normally has a superior and lateral course towards the mental foramen. In some cases, the nerve passes forward anteriorly, hence forming a curve back towards the mental foramen, so called anterior loop. It is the measurement of the anterior extension of the nerve that must be observed carefully, which is sometimes called "length of anterior loop"—a term that may be misleading. Anterior extensions bigger than 2 mm are clinically relevant, especially for implant placement.

The method used to measure the anterior extension of the mental nerve is quite relevant. Conventional radiography may fail to demonstrate the true anatomical shape and extension of the anterior loop [4, 5], especially when poor bone quality is observed [8]. Uchida et al. [10] confirmed CBCT as a reliable tool to determine the anterior extension of the nerve, which showed average discrepancies of 0.06 mm or less when compared to cadaveric anatomic measurements.

In order to measure distances on three-dimensional images, a reference plane must be chosen, which ideally should be clinically reproducible. Previous studies have used the inferior margin of the mandible as reference plane [8, 10]. However, transoperative use of the occlusal plane as a reference seems more logical. In the present study, two reference planes were used for measurement of anterior loop extension: inferior margin of mandible (for measurements on panoramic reconstructions) and occlusal plane (for cross-sections).

Panoramic reconstructions and cross-sections were chosen in this study because the mandibular region where the MF is located is oblique with sagittal and coronal planes. Clinical measurements are generally also carried out following this transverse inclination of the dental arch. Additionally, cross-sectional images are routinely used to present distance measurements for implant planning. Panoramic reconstructed images are generated conforming to a curvilinear plane, which is manually demarcated based on the patient's dental arch. Some software programs provide multiple additional panoramic slices parallel to the central plane, which are positioned closer to the buccal and lingual side. Often this image will provide a reference marker system, corresponding to the perpendicular numbered lines on the axial display and cross-sectional images, providing correlative information, which is very useful for a combined observational strategy.

Agreement between observations on both views regarding presence/extension of anterior loop was substantial. However, uncertainty regarding the presence of anterior loop (decreased visibility) was higher among cross-sections. Presence of anterior loop was not clearly discernible in 11% of cross-sections, which means that discriminating the MC from surrounding medullar spaces posed as a difficulty in such cases. On the other hand, panoramic reconstructions may fail to show the anterior loop in cases where the mental foramen and the loop are relatively distant buccal-lingually. Thinner reconstructed slices (e.g., 0.2 mm) may not be able to display simultaneously the mental foramen and anterior loop, while thicker slices (e.g., 20 mm) may present significant image overlapping. Observation of both cross-sectional and panoramic reconstructions, as well as all other available views, is recommended.

Patient exposure to radiation is certainly a major concern and thus influences on selection of the appropriate imaging technique for preoperative planning. However, it should be stated that the large variation of CBCT radiation doses [27] implies that there is not a straightforward answer when it comes to deciding to use CBCT or not. In fact, one interpretation could be that with effective dose of 50 μSv or less with optimized CBCT exposure protocols, those could be easily contrasted with other imaging techniques. For digital panoramic radiographs, effective dose has been shown to vary from 5 to 24 μSv [25, 26]. An intra-oral full mouth radiographic status with digital radiography may actually fall in the same dose range and up to 110 μSv [26]. Whereas CBCT effective dose may range from 19 to 368 μSv, CBCT scanners, and protocols providing below 50 μSv may present an acceptable dose [27]. Multi-slice computed tomography shows higher effective dose, ranging from 474 to 1,160 μSv [28]. With the protocol and machine used in the present study, the estimated effective dose was 45 μSv, which is equivalent to two to nine digital panoramic radiographs, and at least one tenth of the dose for multi-slice computed tomography.

Recommendations of safe fixed distances from anatomical landmarks for placement of endosseous implants are not reliable [10]. Large variability among individuals regarding neurovascularization of the mandible and limitations of conventional radiography to properly show these anatomical variations [4, 5, 8] point out the valuable contribution of preoperative examination with low-dose CBCT prior to surgical procedures, particularly for implant placement when three-dimensional information is required for evaluation of bone morphology and dimensions, for inspecting local bone conditions and potential pathology, and for biomechanical and esthetic setup.

Acknowledgments Author COS was granted PDEE scholarship—doctorate program with part of studies developed abroad, from CAPES-Brazil (Brazilian Government Agency).

Conflicts of interest The authors declare no conflicts of interest regarding the manuscript and publication of the manuscript and its potential implications.

References

1. Jacobs R, Lambrichts I, Liang X, Martens W, Mraiwa N, Adriaensens P, Gelan J (2007) Neurovascularization of the anterior jaw bones revisited using high resolution magnetic resonance imaging. Oral Surg Oral Med Oral Pathol Oral Radiol Endod 103:683–693
2. Juodzbalys G, Wang H, Sabalys G (2010) Anatomy of mandibular vital structures. Part I: mandibular canal and inferior alveorlar

neurovascular bundle in relation with dental implantology. J Oral Maxillofac Res 1:e2

3. Kilic C, Kamburoglu K, Ozen T, Balcioglu HA, Kurt B, Kutoglu T, Ozan H (2010) The position of the mandibular canal and histologic feature of the inferior alveolar nerve. Clin Anat 23:34–42
4. Mardinger O, Chaushu G, Arensburg B, Taicher S, Kaffe I (2000) Anterior loop of the mental canal: an anatomical-radiologic study. Implant Dent 9:120–125
5. Kuzmanovic DV, Payne AGT, Kieser JA, Dias GJ (2003) Anterior loop of the mental nerve: a morphological and radiographic study. Clin Oral Implants Res 14:464–471
6. Hu KS, Yun HS, Hur MS, Kwon HJ, Abe S, Kim HJ (2007) Branching patterns and intraosseous course of the mental nerve. J Oral Maxillofac Surg 65:2288–2294
7. Uchida Y, Yamashita Y, Goto M, Hanihara T (2007) Measurement of anterior loop length for the mandibular canal and diameter of the mandibular incisive canal to avoid nerve damage when installing endosseous implants in the interforaminal region. J Oral Maxillofac Surg 65:1772–1779
8. Kaya Y, Sencimen M, Sahin S, Okcu KM, Dogan N, Bahcecitapar M (2008) Retrospective radiographic evaluation of the anterior loop of the mental nerve: comparison between panoramic radiography and spiral computerized tomography. Int J Oral Maxillofac Implants 23:919–925
9. Ngeow WC, Dionysius DD, Ishak H, Nambiar P (2009) A radiographic study on the visualization of the anterior loop in dentate subjects of different age groups. J Oral Sci 51:231–237
10. Uchida Y, Noguchi N, Goto M, Yamashita Y, Hanihara T, Takamori H, Sato I, Kawai T (2009) Measurement of anterior loop length for the mandibular canal and diameter of the mandibular incisive canal to avoid nerve damage when installing endosseous implants in the interforaminal region: a second attempt introducing cone beam computed tomography. J Oral Maxillofac Surg 67:744–750
11. Liang X, Jacobs R, Hassan B, Li LM, Pauwels R, Corpas L, Couto Souza P, Martens M, Shahbazian M, Alonso A, Lambrichts I (2010) A comparative evaluation of Cone Beam Computed Tomography (CBCT) and Multi-Slice CT (MSCT)—Part I: on subjective image quality. Eur J Radiol 75:265–269
12. Lew K, Townsend G (2006) Failure to obtain adequate anaesthesia associated wiyh a bifid mandibular canal: a case report. Aust Dent J 51:86–90
13. Nortjé CJ, Farman AG, Grotepass FW (1977) Variations in the anatomy normal of the inferior dental (mandibular) canal: a retrospective study of panoramic radiographs from 3612 routine dental patients. Br J Oral Surg 15:55–63
14. Langlais RP, Broadus R, Glass BJ (1985) Bifid mandibular canals in panoramic radiographs. JADA 110:923–926
15. Sanchis JM, Peñarrocha M, Soler F (2003) Bifid mandibular canal. J Oral Maxillofac Surg 61:422–424
16. Naitoh M, Hiraiwa Y, Aimiya H, Ariji E (2009) Observation of bifid mandibular canal using cone-beam computerized tomography. Int J Oral Maxillofac Implants 24:155–159
17. Kuribayashi A, Watanabe H, Imaizumi A, Tantanapornkul W, Katakami K, Kurabayashi T (2010) Bifid mandibular canals: cone beam computed tomography evaluation. Dentomaxillofac Radiol 39:235–239
18. Chávez-Lomeli ME, Mansilla-Lory J, Pompa JA, Kjær I (1996) The human mandibular canal arises from three separate canals innervating different tooth groups. J Dent Res 75:1540–1544
19. Sawyer DR, Kiely ML (1991) Retromolar foramen: a mandibular variant important to dentistry. Ann Dent 50:16–18
20. Bilecenoglu B, Tuncer N (2006) Clinical and anatomical study of retromolar foramen and canal. J Oral Maxillofac Surg 64:1493–1497
21. Parnia F, Fard EM, Mahboud F, Hafzeqoran A, Gavgani FE (2010) Tomographic volume evaluation of submandibular fossa in patients requiring dental implants. Oral Surg Oral Med Oral Pathol Oral Radiol Endod 109:e32–e36
22. Oliveira-Santos C, Rubira-Bullen IR, Dezzoti MSG, Capelozza ALA, Fischer CM, Poleti ML (2011) Visibility of the mandibular canal on CBCT cross-sectional images. J Appl Oral Sci 19:130–133
23. Lofthag-Hansen S, Gröndahl K, Ekestubbe A (2009) Cone-beam CT for preoperative implant planning in the posterior mandible: visibility of anatomic landmarks. Clin Implant Dent Relat Res 11:246–255
24. Liang X, Jacobs R, Corpas LS, Semal P, Lambrichts I (2009) Chronologic and geographic variability of neurovascular structures in the human mandible. Forensic Sci Int 190:24–32
25. Gijbels F, Jacobs R, Bogaerts R, Debaveye D, Verlinden S, Sanderink G (2005) Dosimetry of digital panoramic imaging. Part I: patient exposure. Dento-Maxillo-Facial Radiol 34:145–149
26. Ludlow JB, Davies-Ludlow LE, White SC (2008) Patient risk related to common dental radiographic examinations: the impact of 2007 international commission on radiological protection recommendations regarding dose calculation. J Am Dent Assoc 139:1237–1243
27. Pauwels R, Beinsberger J, Collaertb B, Theodorakou C, Rogers J, Walker A, Cockmartin L, Bosmans H, Jacobs R, Bogaerts R, Horner K (2011) Effective dose range for dental cone beam computed tomography scanners. Eur J Radiol (in press), doi:10.1016/j.ejrad.2010.11.028
28. Loubele M, Bogaerts R, Van Dijck E, Pauwels R, Vanheusden S, Suetens P, Marchal G, Sanderink G, Jacobs R (2009) Comparison between effective radiation dose of CBCT and MSCT scanners for dentomaxillofacial applications. Eur J Radiol 71:461–468

Copyright of Clinical Oral Investigations is the property of Springer Science & Business Media B.V. and its content may not be copied or emailed to multiple sites or posted to a listserv without the copyright holder's express written permission. However, users may print, download, or email articles for individual use.